Single hydrogen atoms on the Si(001) surface

M. W. Radny,[1] P. V. Smith,[1] T. C. G. Reusch,[2] O. Warschkow,[3] N. A. Marks,[3] H. F. Wilson,[3] S. R. Schofield,[1]
N. J. Curson,[2] D. R. McKenzie,[3] and M. Y. Simmons[2]

[1]*School of Mathematical and Physical Sciences, The University of Newcastle, Callaghan 2308, Australia*
[2]*Centre for Quantum Computer Technology, School of Physics, The University of New South Wales, Sydney 2052, Australia*
[3]*Centre for Quantum Computer Technology, School of Physics, The University of Sydney, Sydney 2006, Australia*

Chemisorption of a single hydrogen atom on the *n*-type Si(001) surface is investigated by scanning tunneling microscopy (STM) and first-principles density functional theory (DFT) calculations. The STM experiments show that the formation of a hemihydride induces static buckling of the neighboring Si-Si dimers and suggest that different buckling configurations of these dimers are observed at negative and positive biases. They also show that the appearance of an isolated Si-Si-H hemihydride on Si(001) exhibits a complex voltage dependence with the brightness of the dangling bond of the hemihydride changing significantly at negative sample bias. DFT calculations predict two stable, ground state atomic configurations for the hemihydride on Si(001). These correspond to parallel and antiparallel configurations of the Si-Si-H hemihydride with respect to the neighboring bare Si-Si dimers. In order to understand the bias-dependent appearance in the STM images of the *n*-type Si(001) surface, we include the effect of hemihydride charging due to tip-induced band bending. In filled state, the STM images are shown to result from the electronic and structural features that originate from the charge-dependent parallel configuration. In empty state, the energetics and STM measurements support the charge independent antiparallel configuration, while either structure can produce simulated images consistent with experiment.

PACS number(s): 68.35.Bs, 68.43.−h

I. INTRODUCTION

One of the most important characteristics of semiconductor surfaces is the existence of dangling bonds. Semiconductor surfaces undergo reconstruction in order to minimize the number of surface dangling bonds, and it is the dangling bonds remaining after the reconstruction that determine both the chemical reactivity and the electronic properties of the surface. Modification of the electronic and chemical properties of semiconductor surfaces is also generally achieved by the adsorption of adatoms at the chemically active dangling bond sites.[1]

Hydrogenation is a simple, yet effective, way to chemically passivate semiconductor surfaces by saturating the dangling bonds.[1] This observation has led to the hydrogen-terminated substrate emerging as an important template for the chemisorption-assisted functionalization of semiconductor surfaces. This is due to the demonstrated ability of scanning tunneling microscopy (STM) to produce patterns of reactive areas by selectively desorbing hydrogen atoms from the completely hydrogenated surface.[2–4]

The effect of hydrogenated Si-Si dimers on the structural and electronic properties of residual dangling bonds on Si(001) has already been investigated.[5] In particular, the electronic structure of the smallest possible reactive area, an isolated Si dimer dangling bond resulting from the absence of just one hydrogen atom, has been studied using STM and scanning tunneling spectroscopy (STS).[6–9] This electronic structure has been interpreted in terms of two dangling bond states near the Fermi energy (E_F) that can contribute to the tunneling. STS measurements for the Si(001) surface have confirmed this interpretation and revealed two peaks in the density of states near E_F at −0.4 and +0.2 eV.[6] Measure-

ments by Bobrov *et al.*[10] using valence band photoemission determined the energy of the occupied dangling bond level to be 0.7 eV below E_F.

In this paper, we focus on the properties of an isolated Si dimer dangling bond formed by the chemisorption of a single hydrogen atom onto an otherwise perfectly clean Si(001) surface. Adsorption of a single hydrogen atom breaks the Si-Si dimer π bond and forms a Si-Si-H hemihydride.[7] This creates an isolated dangling bond on the free Si atom of the hemihydride. Schematic representations of a bare Si-Si dimer and a Si-Si-H hemihydride with their associated dangling bonds are shown in Figs. 1(a) and 1(b), respectively. In contrast to Refs. 5–9, where an isolated Si dimer dangling bond surrounded by *fully hydrogenated* Si-Si dimers (monohydrides) was investigated, we study the effect of the surrounding *bare* Si-Si dimers on the structural and electronic properties of the isolated dangling bond of a single Si-Si-H hemihydride.

Previously reported STM experiments of hemihydrides on the Si(001) surface show them as a bright protrusion and a depression on opposite sides of a single dimer in both filled and empty state imaging.[8,9,11,12] We present detailed STM
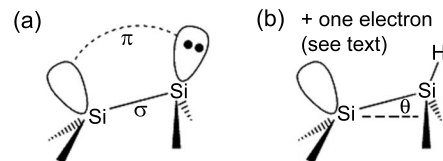

FIG. 1. Schematic of (a) a Si-Si dimer and (b) a Si-Si-H hemihydride. Each filled circle denotes occupancy by an electron. The lobes represent the dangling bond states and θ denotes the buckling angle of the Si-Si-H hemihydride.

data and show that the appearance of an isolated Si-Si-H hemihydride is not simple but displays complex voltage dependence in STM imaging. Based on *ab initio* density functional theory (DFT) calculations, we demonstrate that the adjacent, bare Si-Si dimers have a pronounced effect on both the geometry and electronic structure of a hemihydride. We find that there are two stable structures for an isolated hemihydride on Si(001). This finding agrees with the results of a recently published study on the interaction between hemihydrides on a small (2×2) model Si(001) surface by van Heys and Pehlke.[13] Contrary to this latter work, however, we find that for the two identified configurations, the unpaired electron is delocalized on the surface, rendering the isolated Si dangling bond of the hemihydride unoccupied. Comparison of the theoretical simulations with the experimental STM data yields two additional important findings: (i) the appearance of the isolated hemihydride changes with negative bias voltage due to the local charging, and (ii) while the empty state images could arise from either of the two configurations, the structure that is observed in the filled state STM images originates from the charge-dependent parallel configuration. These findings are similar to the results that were obtained in our earlier theoretical and STM studies of the interaction of phosphorus with the Si(001) surface.[14] The results reported in this paper are thus relevant to many other systems in which an isolated dangling bond is formed on the Si(001) surface.[15]

II. EXPERIMENTAL AND COMPUTATIONAL METHODOLOGY

All experiments were performed in an UHV Omicron variable temperature scanning tunneling microscope at a base pressure of 2×10^{-11} mbar. The STM tips were etched from polycrystalline tungsten wire and outgassed for a couple of hours at 150 °C before the measurement. All STM measurements were performed at room temperature.

The samples were cleaved from polished Si(001) wafers doped with P (*n* type) to a resistivity of around 1 Ω cm. Clean Si(001) surfaces were prepared by outgassing the samples at temperatures around 550 °C for a couple of hours and flashing in UHV for 20 s at 1100 °C, followed by a controlled cool down from 900 °C to room temperature of approximately 2 °C/s. Sample heating was achieved by passing a current directly through the sample. The substrate temperature was measured with an infrared pyrometer. The pressure during flashing and cool down did not exceed 1 $\times 10^{-10}$ mbar.

Atomic hydrogen was provided by cracking ultrapure (99.9999%) molecular hydrogen on a heated tungsten filament with a water-cooled heat shroud. Single hydrogen atoms were adsorbed to the Si(001) surface by exposure at room temperature to typically 6.3×10^{-3} L (1 L $=10^{-6}$ Torr s) of atomic hydrogen from a cracker cell.

The VASP computer code[16–18] has been employed to carry out the geometry optimizations and electronic structure calculations that are reported in this study. This method is based on DFT and employs pseudopotentials and a plane wave basis set. The calculations have been carried out using Vander-

bilt ultrasoft pseudopotentials.[19] All of the results have been obtained using fully spin polarized calculations in which the up and down spins are allowed to be distinct. The generalized gradient approximation PW91 functional was used for exchange and correlation.[20] Most of the calculations have been carried out using a (4×4) surface unit cell, slabs containing either four or six Si layers, a vacuum region of ~ 10 Å, and a terminating hydrogen layer. This terminating layer was kept fixed, as well as at least one of the adjacent Si layers. The total energy calculations were performed using our determined bulk lattice constant of 5.456 Å and four **k** points in the irreducible symmetry element of the surface Brillouin zone (SBZ). Additional calculations have been performed using (2×4), (2×6), and (6×6) surface unit cells.

The STM images have been simulated from the VASP calculations using the Tersoff-Hamann approximation.[21,22] Under this approximation, the intensity of a constant-current STM image is modeled by integrating the local density of state function [to obtain an integrated local density of state (ILDOS) plot] over an energy range of $\pm X$ eV from the Fermi energy (such images are subsequently referred to as the $\pm X$ eV simulated images). Our simulated STM images thus correspond to *xyz* plots in which the height *z* associated with tracing out a selected ILDOS isosurface value is converted into a gray scale. All of the ILDOS plots in this paper have been presented for the isosurface value of 2.7 $\times 10^{-4}$ $e/$Å^3. This corresponds to a distance of approximately 4.0 Å above the surface, which is a reasonable value given that the density functional theory generally overestimates the decay of the wave functions into the vacuum. Moreover, the qualitative features of the ILDOS plots are relatively insensitive to the isosurface value that is employed.

The electronic band structures for the two theoretically predicted Si-Si-H configurations have been determined by calculating the eigenenergies for each structure at 30 **k** points along the Γ-*J*-*K*-*J'*-Γ-*K* symmetry directions of the 4×4 SBZ.

III. RESULTS

A. Scanning tunneling microscopy data and structure assignment

Figures 2(a)–2(e) show voltage-dependent STM topographs for a Si-Si-H hemihydride on an *n*-type Si(001) substrate. Enlarged images are presented in panels (g) and (h) where we have overlaid a close-up from the topographic images in panels (c) and (e), respectively, with a structure schematic. The images in Figs. 2(a)–2(d) were obtained using a set point current of 114 pA, while that of Fig. 2(e) corresponds to a current of 99 pA. This slight change in current is inconsequential as one usually has to vary currents by an order of magnitude to produce any significant effect on the STM images.

Examination of Figs. 2(a)–2(e) shows that the hemihydride dangling bond displays a complex bias dependence in STM imaging. For high filled state bias [Fig. 2(c), $U=$ -2.2 V], the feature appears as a bright asymmetric elevation on a dimer with static buckling of the neighboring Si-Si
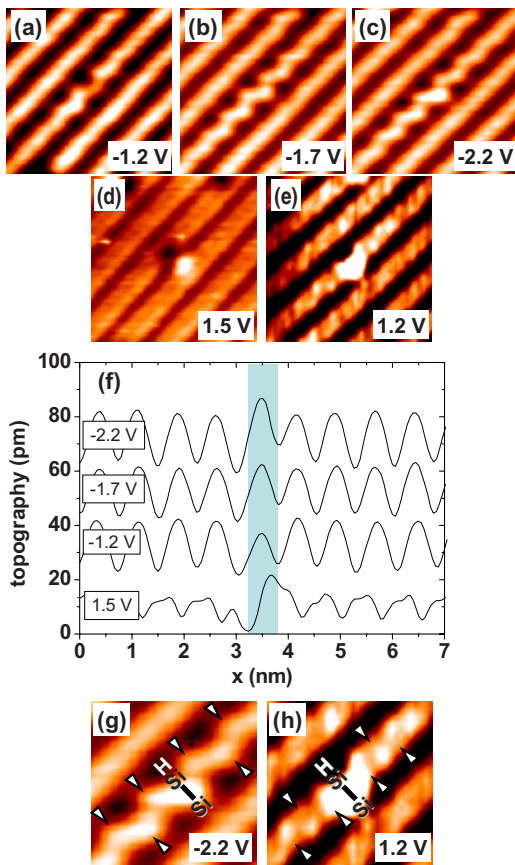
FIG. 2. (Color online) [(a)–(e)] Voltage-dependent STM measurements of a Si-Si-H hemihydride feature for an *n*-type doped Si(001) surface. The sample voltages are indicated. (f) Line profiles through the hemihydride perpendicular to the dimer rows and displayed from the upper left to the lower right. The dangling bond site is indicated by the shading. Each trace has been offset vertically for clarity. [(g) and (h)] Magnified views of the hemihydride in panels (c) and (e) overlaid with a schematic of the hemihydride. Up-buckled Si atoms are indicated by the arrows. These assignments of the up-buckled Si atoms are based on the assumption that it is the up-buckled Si atoms that appear bright in filled state images, and the down-buckled Si atoms in empty state images.
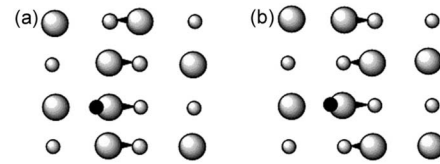

FIG. 3. Schematics of the (a) parallel HH1 and (b) antiparallel HH2 Si-Si-H hemihydride configurations on the Si(001) surface. The large shaded circles indicate an up-Si atom and the small shaded circles denote the down-Si atoms. The hydrogen atom of the hemihydride is represented by the small filled circle.

dimers. Decreasing the bias to $U=-1.7$ V [Fig. 2(b)], the brightness of the hemihydride is diminished and for $U=-1.2$ V [Fig. 2(a)], the hemihydride appears darker than the surrounding buckled Si-Si dimers. At empty state bias [Figs. 2(d) and 2(e)], the hemihydride appears as an elevation and a depression along a dimer, with the bright region being on the same end of the dimer as for the filled states. At low empty state bias [Fig. 2(e), $U=+1.2$ V], the top of the dimer rows appears bright, while at higher empty state bias [Fig. 2(d), $U=+1.5$ V], the weight has shifted toward the trenches in between the dimer rows.[23] In addition, static buckling of the neighboring Si-Si dimers is visible for the low empty state bias in Fig. 2(e). The bias dependence of the apparent height of the bare Si atom of the hemihydride in filled state is also clearly evident in the line profiles shown in Fig. 2(f). These line profiles were taken perpendicular to the dimer rows, intersecting the hemihydride over the range indicated by the

shading. All of the above-mentioned transitions are fully reversible with bias and have been observed using different tips and samples. The bright appearance of the hemihydride feature in the higher-voltage filled and empty state STM images has previously been explained as being due to the creation of a singly occupied dangling bond on the unsaturated Si atom. However, single occupancy of the dangling bond cannot explain the complex bias-dependent transition that is observed between the filled state images shown in Figs. 2(a)–2(c).

The formation of a hemihydride is seen to induce static buckling of the neighboring Si-Si dimers. The common interpretation of bias-dependent STM images on Si(001) is that the up-buckled Si atoms image brightly in filled state and the down-buckled atoms appear bright in empty state.[23,24] Based on this interpretation, we have indicated by arrows the up-buckled Si atoms in the enlarged filled state image of Fig. 2(g). The Si-Si dimers are seen to be buckled such that the up-buckled Si atoms of the immediately adjacent Si-Si dimers are on the *opposite* side of the dimer row to the non-hydrogenated Si atom of the Si-Si-H. By contrast, the neighboring Si-Si dimers to the hemihydride in the empty state image of Fig. 2(h) appear to be buckled with their up-Si atoms (again indicated by arrows) on the *same* side of the dimer row as the nonhydrogenated Si atom of the Si-Si-H. This observation suggests a change in the buckling configuration with the bias in the STM experiment.

Our total energy DFT calculations show that there are indeed two stable configurations for an isolated Si-Si-H hemihydride on a Si(001) surface. In both of these structures, the nonhydrogenated Si atom of the Si-Si-H is always the down atom [see Fig. 1(b)]. The two structures differ in the buckling configurations of their neighboring Si-Si dimers: in one configuration, the buckling angles of the adjacent Si-Si dimers have the same sign as the buckling angle of the hemihydride (parallel configuration, HH1), and in the other, the buckling angle of the hemihydride has the opposite sign to its two neighboring Si-Si dimers in the same dimer row (antiparallel configuration, HH2). These two configurations are shown in Figs. 3(a) and 3(b), respectively. Van Heys and Pehlke[13] calculated the energy difference between the HH1 and HH2 configurations to be 0.011 eV, which was within the error of their calculations, and hence they concluded that these structures were isoenergetic. Our (4×4) and (6×6) surface unit cell calculations predict the converged energy difference between these two configurations to be ~ 0.13 eV, with the antiparallel HH2 configuration being the lower-energy structure.

TABLE I. Calculated dimer buckling angles (in deg) and bond lengths (in Å, given in parentheses) of the Si-Si-H hemihydride and the nearest (n) and next-nearest (nn) Si-Si dimer, as a function of surface unit cell size. E(HH2)-E(HH1) is the calculated energy difference between the HH2 and HH1 configurations in eV per surface unit cell.

	Dimer	(2×2)[a]	(2×4)	(2×6)	(4×4)	(6×6)
HH1	Si-Si-H	+2	+0.6 (2.41)	+1.4 (2.42)	+1.9 (2.41)	+8.5 (2.39)
	Si-Si (n)		+18.0 (2.34)	+18.4 (2.36)	+18.2 (2.35)	+18.6 (2.35)
	Si-Si (nn)		−18.5 (2.36)	−18.8 (2.38)	−18.7 (2.38)	−18.7 (2.37)
HH2	Si-Si-H	+5	+9.4 (2.37)	+9.0 (2.38)	+9.6 (2.39)	+9.9 (2.39)
	Si-Si (n)		−19.1 (2.35)	−19.2 (2.37)	−19.1 (2.37)	−19.0 (2.37)
	Si-Si (nn)		+19.5 (2.37)	+19.4 (2.38)	+19.5 (2.38)	+19.0 (2.37)
E(HH2)-E(HH1)		−0.011	−0.040	−0.097	−0.134	−0.128

[a]Reference 13.

Based on the above total energy calculations, one would expect to find the experimental STM topographs of an isolated hemihydride on a bare Si(001) surface to be consistent with the HH2 configuration of alternately buckled dimers [see Fig. 3(b)]. Close inspection of the expanded STM images in Figs. 2(g) and 2(h) with their assigned up- and down-Si dimer atoms, however, reveals that while it is the lower-energy antiparallel HH2 configuration [Fig. 3(b)] that is in agreement with the empty state image of Fig. 2(h), it is clearly the structure that originates from the higher-energy parallel HH1 configuration [Fig. 3(a)] that is observed in the high negative bias voltage filled state image of Fig. 2(g). As we will show, the simulated STM images based on the simple Tersoff-Hamann approximation fully confirm this structure assignment for the filled states but are inconclusive for the empty state images. In order to understand the reasons for this, we need to consider the details of the atomic and electronic structures of the HH1 and HH2 configurations.

B. Atomic and electronic structure

1. Atomic configurations

The structural characteristics of the HH1 and HH2 configurations calculated for different sizes of the surface unit cell are presented in Table I. The bond lengths of the Si-Si dimers adjacent to the hemihydride were found to be very similar for both the HH1 and HH2 configurations, independent of the size of the surface unit cell. The buckling angles and bond lengths of the neighboring Si-Si dimers for both the HH1 and HH2 configurations are quite similar to those of the Si-Si dimers on the clean Si(001) surface ($\sim19°$ and 2.4 Å). The buckling angles of the Si-Si(H) dimers, on the other hand, are seen to be significantly less than the buckling angles of the neighboring Si-Si dimers for both the HH1 and HH2 configurations. For the antiparallel HH2 configuration, a buckling angle of $\sim9.5°$ is obtained, independent of the size of the unit cell. By contrast, for the parallel HH1 orientation, the size of the unit cell leads to different buckling angles for the hemihydride with the (2×4), (2×6), and (4×4) unit cells giving small buckling angles of $0.6°$–$1.9°$,

while for the (6×6) surface unit cell, a buckling angle of $8.5°$ was obtained. This abrupt increase in the buckling angle of the Si-Si-H hemihydride, when going from a (4×4) to a (6×6) surface unit cell, is related to the localization of the unpaired electron as we shall discuss later. It should be noted that the results reported in Table I (and subsequently) for the (6×6) surface unit cell were obtained using Γ-point sampling. Employing four special **k** points in the irreducible symmetry element of the SBZ for the (6×6) surface unit cell gave buckling angles for the Si-Si-H hemihydride in the HH1 and HH2 configurations of $7.3°$ and $9.6°$, respectively, and an energy difference between these two configurations of $−0.136$ eV.

Similar structures to our HH1 and HH2 configurations for Si-Si-H hemihydrides were recently obtained from studies of the adsorption of single hydrogen atoms on Si(001) in the limit of a small (2×2) surface unit cell.[13] The buckling angle of $2°$ determined by van Heys and Pehlke[13] for the HH1 configuration is in good agreement with our (2×4), (2×6), and (4×4) results. However, the value of $5°$ obtained by van Heys and Pehlke[13] for the buckling angle of the hemihydride in the HH2 configuration using a (2×2) unit cell is significantly less than our values of $\sim9.5°$.

2. Electronic structures

Both the HH2 and HH1 configurations have one unpaired electron which is shared with the surface atoms. van Heys and Pehlke[13] predicted that this electron would occupy the isolated dangling bond orbital of the hemihydride in both configurations leading to a metallic state for these systems. We will show that this intuitive prediction is incorrect. The different arrangements of the buckled Si-Si dimers adjacent to the hemihydride for the HH1 and HH2 configurations result in two rather different electronic structures and hence quite different behaviors of the unpaired electron in the two cases. In particular, we will show that the electronic structure of the HH1 configuration is sensitive to the surface charge density.

a. HH2 configuration. The surface electronic band structures near E_F for the clean Si(001) surface and the minimum energy HH2 configuration for a (4×4) surface unit cell are
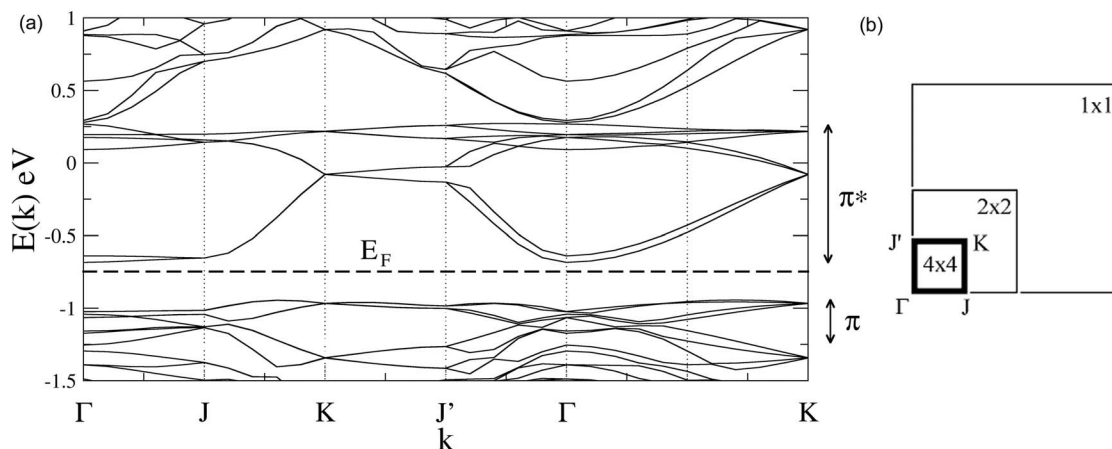
FIG. 4. (a) The surface electronic structure of the clean Si(001) surface calculated for a (4×4) surface unit cell with six Si layers in the vicinity of the Fermi level E_F (indicated by the dashed horizontal line). The vertical arrows indicate the occupied (π) and unoccupied (π^*) bands of surface electronic states of predominantly up-Si and down-Si dimer atom characters, respectively. The low-energy surface states within the π^* band are dispersive along the dimer row (J-K and J'-Γ directions) and flat (localized) in the direction perpendicular to the dimer rows (Γ-J and K-J' directions). The upper part of the π^* band consists of fairly dispersionless states associated with the isolated down-Si atom. (b) The irreducible symmetry element of the (4×4) SBZ.

shown in Figs. 4(a) and 5(a), respectively. Each band is doubly degenerate in these band structures because the energies of the corresponding majority- and minority-spin states are the same for these systems. The energies of the filled Si–H bonding and empty Si–H antibonding orbitals lie more than 2.0 eV from the Fermi level and hence do not appear in the HH2 band structure in Fig. 5(a). The hemihydride in the HH2 configuration thus gives rise to a surface electronic structure in the vicinity of E_F that is fairly similar to that of the clean Si(001) surface shown in Fig. 4(a). The only evident differences between the calculated electronic structure for the HH2 configuration [Fig. 5(a)] and that for the clean Si(001) surface [Fig. 4(a)] arise from the two states denoted in Fig. 5(a) by the empty circles and the filled squares. For the clean Si(001) surface, these bands lie at the top and bottom, respectively, of the unoccupied π^* surface state band.

For the HH2 configuration, both of these states are shifted down relative to the Fermi energy so that the lower (filled square) state becomes partially occupied by the unpaired electron.

The flat, dispersionless surface state above E_F, denoted by the empty circles in Fig. 5(a), is characterized by a three-dimensional probability density distribution that is localized primarily on the down-Si atom of the Si-Si-H hemihydride. By contrast, the filled square surface state is seen to exhibit significant dispersion along the J-K and J'-Γ symmetry directions and negligible dispersion along the Γ-J and K-J' symmetry directions. It is thus expected that the charge associated with the unpaired electron will be delocalized along the dimer row and strongly localized in the direction perpendicular to the dimer row.
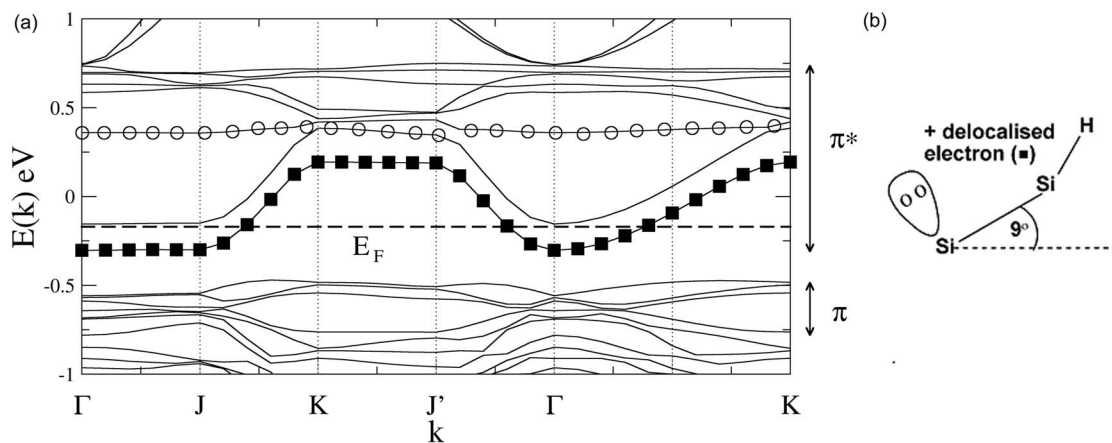

FIG. 5. (a) The surface electronic structure of the HH2 Si-Si-H configuration calculated using a (4×4) surface unit cell with six Si layers in the vicinity of the Fermi level E_F (indicated by the dashed horizontal line). The empty circles and filled squares denote surface states intrinsic to the Si(001) substrate that are significantly affected by the chemisorption of a H atom onto one of the Si-Si dimers. The filled squares denote the surface state partially occupied by the delocalized, unpaired electron. (b) Schematic of the HH2 ground state configuration. The empty circles denote the absence of an electron.
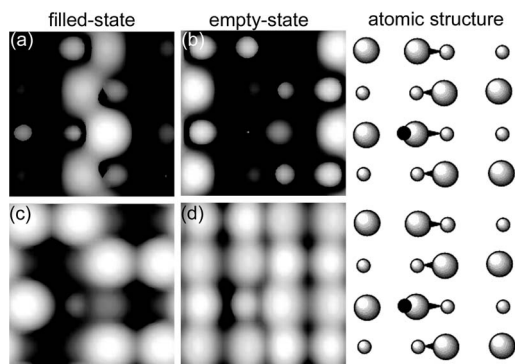
FIG. 6. Integrated LDOS for the HH2 Si-Si-H configuration for a (4×4) surface unit cell. Range of integration from the Fermi energy: (a) −0.2 eV, (b) +0.2 eV, (c) −1.0 eV, and (d) +1.0 eV. The isosurface value was 2.7×10^{-4} $e/\text{Å}^3$. The right hand panels indicate the buckling of the Si-Si dimers and the Si-Si-H hemihydride within the (4×4) surface unit cell. The large shaded circles indicate an up-Si atom and the small shaded circles denote the down-Si atoms. The hydrogen atom of the hemihydride is represented by the small filled circle.

The spatial extent of the unpaired electron can best be seen from the calculated local density of electronic states (LDOS) integrated over the range of ±0.2 and ±1.0 eV from the Fermi level. These ILDOS plots show the spatial distribution of the surface energy bands within the adopted range of integration and are shown in Fig. 6 for a (4×4) surface unit cell. The bright features in the filled state plots (left side of Fig. 6) denote regions of high charge density. Figure 6(a) corresponds to an integration range of −0.2 eV and hence only includes contributions from the band that crosses the Fermi energy [filled squares in Fig. 5(a)]. As expected, the unpaired electron is seen to be strongly localized in the direction perpendicular to the dimer rows but is delocalized along the dimer row containing the hemihydride. By comparison, the plot in Fig. 6(c) for −1.0 eV (which contains all of the occupied surface states within 1.0 eV of E_F) shows that the only really bright features are those associated with the doubly occupied dangling bonds of the up-buckled atoms of the bare Si-Si dimers, and the unsaturated hemihydride Si atom appears relatively dark. This confirms that the unpaired electron is not present in the dangling bond orbital at this site. Identical features can also be identified in the electronic band structure calculated for the HH2 configuration for a
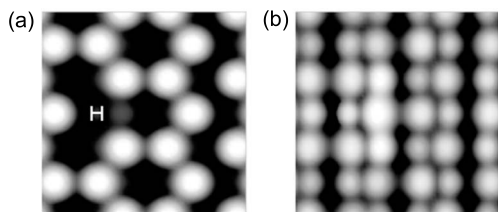

FIG. 7. ILDOS for the HH2 Si-Si-H configuration for a (6 ×6) surface unit cell. Range of integration from the Fermi energy: (a) −1.0 eV and (b) +1.0 eV. The isosurface value was 2.7 $\times 10^{-4}$ $e/\text{Å}^3$.
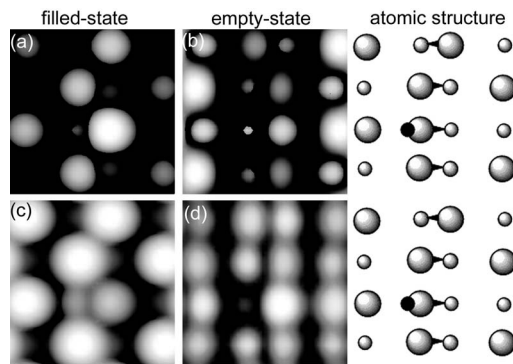

FIG. 8. Integrated LDOS for the HH1 Si-Si-H configuration for a (4×4) surface unit cell. Range of integration from the Fermi energy: (a) −0.2 eV, (b) +0.2 eV, (c) −1.0 eV, and (d) +1.0 eV. The plots are for the isosurface value of 2.7×10^{-4} $e/\text{Å}^3$. The right hand panels indicate the buckling of the Si-Si dimers and the Si-Si-H hemihydride within the (4×4) surface unit cell. The large shaded circles of the hemihydride are represented by the small filled circles.

(6×6) unit cell. Due to folding of the bands, however, this band structure is much more complicated and difficult to analyze than for a (4×4) surface unit cell and hence is not shown. The ILDOS plots for ±1.0 eV for an isolated Si-Si-H hemihydride in the HH2 configuration for the (6×6) surface unit cell are presented in Fig. 7. It is clear that Fig. 7 shows the same qualitative behavior as Fig. 6. Moreover, comparison of the plots in Figs. 6(c) and 7(a) shows that the unsaturated Si atom of the hemihydride appears equally dark in both images confirming that the unpaired electron is again delocalized on the surface. This is contrary to the prediction by van Heys and Pehlke.[13]

b. HH1 configuration. The spatial distribution of the unpaired electron for the nearly flat hemihydride in the HH1 configuration calculated using a (4×4) surface unit cell is illustrated by the ILDOS plots in Fig. 8. The ILDOS plot shown in Fig. 8(a) corresponds to an integration range of −0.2 eV and hence only includes contributions from the surface states lying just below E_F. The dominating bright feature in Fig. 8(a) is clearly seen to be localized on the unsaturated hemihydride Si atom. The ILDOS plot for −1.0 eV [Fig. 8(c)] also shows a bright feature at this hemihydride Si atom site. Both of these features are brighter than those obtained for the HH2 configuration [Figs. 6(a), 6(c), and 7(a)]. This brighter appearance is due to the fact that the unpaired electron is mostly localized on the dangling bond orbital of the nonhydrogenated Si atom of the hemihydride for the HH1 configuration.

The predicted charge localization for the HH1 hemihydride configuration can be delineated further from the electronic band structure calculated for a (4×4) unit cell, shown in Fig. 9. This band structure comprises separate minority-spin and majority-spin energy bands. The topologies of the surface state bands for these two spin states are observed to be fairly similar and are again generally similar to the electronic structure of the clean Si(001) surface [see Fig. 4(a)]. The minority- and majority-spin structures do differ signifi-
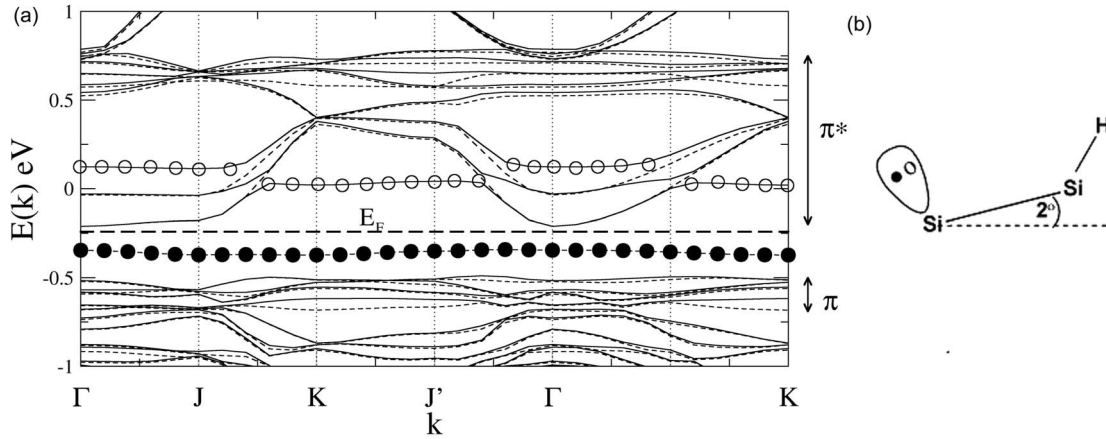
FIG. 9. (a) The surface electronic structure of the HH1 Si-Si-H configuration calculated using a (4×4) surface unit cell with six Si layers in the vicinity of the Fermi level (E_F). The majority-spin and minority-spin bands are indicated by the dashed and solid lines, respectively. The empty and filled circles indicate the hemihydride Si atom dangling bond state that splits into occupied and unoccupied spin states when populated by the unpaired electron. (b) Schematic of the HH1 ground state configuration.

cantly, however, in the location of the two localized, dispersionless surface states in the vicinity of E_F, with one state being below E_F and therefore occupied [filled circles in Fig. 9(a)—majority spin], while the second lies above E_F and is empty [empty circles in Fig. 9(a)—minority spin]. Both of these surface states have their charge/probability densities strongly localized on the down-Si atom of the Si-Si(H) dimer, similar to the empty localized state for the HH2 configuration [see Fig. 5(a)]. In contrast to the HH2 band structure, however, there is no surface state crossing the Fermi level. These observations confirm that for the HH1 configuration, the charge of the unpaired electron is mostly localized on the dangling bond orbital of the down-Si atom of the Si-Si-H hemihydride [Figs. 8(a) and 8(c)] giving rise to the almost flat (buckling angle ~2°) hemihydride geometry. The charge localization also leads to a splitting of the two different spin states associated with the isolated dangling bond level resulting in the semiconducting state of the system. This result is also contrary to the prediction of van Heys and Pehlke[13] that localization of the unpaired electron on the hemihydride dangling bond would lead to a metallic state for the system. Entirely similar results to the above (4×4) results have been obtained for the HH1 hemihydride configurations for (2×4) and (2×6) surface unit cells. Calculations performed for the (6×6) surface unit cell, however, yielded a quite different behavior.
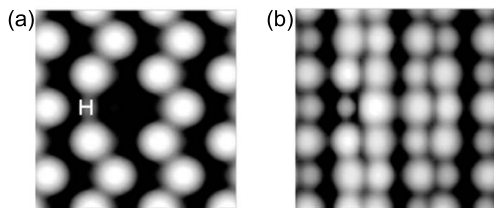

FIG. 10. ILDOS plots for the HH1 Si-Si-H configuration for a (6×6) surface unit cell. Range of integration from the Fermi energy: (a) −1.0 eV and (b) +1.0 eV. The isosurface value was 2.7 $\times 10^{-4}$ $e/\text{Å}^3$.

The spatial distribution of the unpaired electron for the HH1 structure calculated using a (6×6) surface unit cell is illustrated by the ILDOS plot in Fig. 10(a) for −1.0 eV (which again contains all of the occupied surface states within 1.0 eV of E_F). This plot shows that the only really bright features are those associated with the doubly occupied dangling bonds of the up-buckled atoms of the bare Si-Si dimers, and the unsaturated hemihydride Si atom appears dark. This shows that the unpaired electron in a Si(001) surface with a (6×6) periodicity is not present in the dangling bond orbital at this site. This is contrary to the results obtained for the (2×4), (2×6), and (4×4) surface unit cells, where the unpaired electron was found to be localized on the dangling bond of the Si-Si-H hemihydride. This result is also contrary to the prediction of van Heys and Pehlke[13] that the unpaired electron would be localized on the hemihydride dangling bond.

A decrease in the unit cell size from 6×6 to 4×4 (or smaller) is equivalent to a higher hemihydride coverage. This increases the density of unpaired electrons on the surface and, as shown in Table I, leads to a reduction in the HH1 hemihydride buckling angle. This behavior indicates charging of the hemihydride [compare Figs. 8(c) and 10(a)] and suggests that it is the increase in the density of additional electrons that forces them to localize on the hemihydride Si site.

In order to investigate how the density of surface charge modifies the geometry of the hemihydrides, we have carried

TABLE II. Hemihydride buckling angles (in deg) and bond lengths (in Å, given in parentheses) calculated for the HH1 and HH2 configurations for a (4×4) surface unit cell with one less electron ($N_e - 1$) and zero (N_e), one ($N_e + 1$), and two ($N_e + 2$) additional electrons.

	$N_e - 1$	N_e	$N_e + 1$	$N_e + 2$
HH1	9.5 (2.40)	1.9 (2.41)	−1.0 (2.44)	−7.9 (2.47)
HH2	10.0 (2.36)	9.6 (2.34)	10.5 (2.38)	10.7 (2.37)

out geometry optimizations of the HH1 and HH2 configurations for a (4×4) surface unit cell containing one less electron. We denote these electron-deficient systems as N_e-1, where N_e is the number of electrons for the neutral system. In all our calculations, any depletion (or addition) of charge has been compensated by a uniform background. The calculated buckling angles and bond length values of the N_e-1 hemihydride configurations following relaxation are presented in Table II. The geometry of the HH2 hemihydride is observed to be essentially unaffected by the depletion of charge. By contrast, the HH1 configuration changes from a small downward buckling of the unsaturated hemihydride Si atom of 1.9° in the N_e case to 9.5° for the N_e-1 case. This latter buckling angle is quite similar to the value of 8.5° obtained from our N_e (6×6) unit cell calculations (see Table I). These results clearly show that reducing the charge density in the (4×4) surface unit cell leads to a decrease in the HH1 hemihydride buckling angle and an increase in its bond length, analogous to that produced by the lower density of charge on the (6×6) surface.

We would also like to point out that the ability of the HH1 system to localize electrons and decouple the two different spin states associated with the isolated dangling bond level [see Fig. 9(a)] is very similar to that of an unpaired dangling bond on the fully hydrogenated Si(001) surface where two dangling bond electronic states near E_F have been reported.[6–9] Our calculated Kohn-Sham energy of the occupied dangling bond level for the HH1 configuration relative to E_F, however, is only $\sim$−0.1 eV. This is significantly smaller than the corresponding value of $\sim$−0.4 eV for the isolated dangling bond state on hydrogenated Si(001). This difference is most likely due to the presence of the neighboring monohydrides in the latter case.

C. Interpretation of scanning tunneling microscopy images

1. Ground state configurations

a. HH2 ground state configuration. According to the Tersoff-Hamann approximation, the observed filled and empty state STM images presented in Fig. 2 can be compared directly with the ILDOS plots when all the surface bands that are important for imaging are included. Figure 6 (4×4 cell) and Fig. 7 (6×6 cell) thus represent simulated filled and empty state STM images for the HH2 configuration. Comparison of the HH2 −1.0 eV simulated STM images [Figs. 6(c) and 7(a)] with the experimental STM topographs in Figs. 2(a)–2(c) [and the enlargement in Fig. 2(g)] shows that the bright features associated with the up-Si atoms of the Si-Si dimers do not match the static buckling of the Si-Si dimers, which is observed on either side of the Si-Si-H hemihydride in the experimental images. The filled state STM images simulated for the HH2 configuration (which is the lowest energy ground state structure) are therefore not consistent with the experimental data for the low negative voltage. In the +1.0 eV empty state simulated images shown in Figs. 6(d) and 7(b), the nonhydrogenated Si atom of the Si-Si-H is observed to be quite bright and significantly brighter than its counterpart for filled state images. This is consistent with the experimental STM images. How-

ever, the up-buckled Si atoms of the neighboring Si-Si dimers in our simulated images appear to be slightly brighter than the corresponding down atoms.[25] The resultant image is thus characterized by the hemihydride and its two adjacent Si-Si dimers appearing bright on the same side of the dimer row. This is somewhat different to the arrowhead-like experimental empty state image shown in Figs. 2(c) and 2(h).

b. HH1 ground state configuration. The simulated filled and empty state STM images for −1.0 eV for the HH1 ground state configuration are shown in Figs. 8(c), 8(d), and 10. Comparison of the filled state images [Figs. 8(c) and 10(a)] with the experimental STM images in Fig. 2 shows that the bright features associated with the up-Si atoms of the neighboring Si-Si dimers match the static buckling of the Si-Si dimers observed on either side of the Si-Si-H hemihydride in the experimental filled state images. The brightness of these up-Si dimer atoms is also seen to be greater than that of the nonhydrogenated Si atom of the hemihydride in agreement with the low-bias filled state STM experimental images [see Fig. 2(a)]. These results lead us to conclude that it is the HH1 configuration that is observed in STM images of the *n*-type Si(001) surface at relatively low negative bias voltage. On the other hand, the +1.0 eV simulated empty state STM images shown in Figs. 8(d) and 10(b) are observed to be very bright at the site of the unsaturated hemihydride Si atom. The up- and down-buckled Si atoms of the Si-Si dimers are also seen to appear as protrusions of similar magnitude. This is different to the case for the antiparallel HH2 configuration, where the up-buckled Si atoms of the neighboring dimers were predicted to be brighter than the corresponding down atoms [see Figs. 6(d) and 7(b)]. The simulated images in Figs. 8(d) and 10(b) thus seem to be in better agreement with the experimental empty state STM images shown in Figs. 2(e) and 2(h) than the corresponding HH2 simulated images presented in Figs. 6(d) and 7(b).

The STM image shown in Fig. 2(a) also suggests that the brightness of the up-Si atoms of the bare Si-Si dimers is greater than that of the nonhydrogenated Si atom of the hemihydride. On the other hand, the brightness of the nonhydrogenated Si atom site of the hemihydride is greater than the down-Si atoms of the bare Si-Si dimers. Thus, as the dangling bond orbitals on the up-Si dimer atoms are nominally occupied by two electrons, and the down-Si dimer atom dangling orbitals are empty, we conclude that the HH1 configuration that is observed in our STM images of the *n*-type Si(001) surface at relatively low negative bias voltage corresponds to the single unpaired electron being localized on the dangling bond orbital of the nonhydrogenated Si atom [as shown in Fig. 8(a) for the HH1 configuration in a (4 $\times$ 4) unit cell]. While the ground state configuration of the isolated HH1 hemihydride on Si(001) is given by the structure reproduced in our (6×6) unit cell calculations—with the hemihydride dangling bond empty—we have also shown that this decoupled, isolated orbital can act as an attractive center for trapping surface electrons if their surface density is large enough. It has been established that an isolated, decoupled dangling bond on a completely hydrogenated *n*-type Si(001) surface can be occupied by electrons if the doping of the substrate is sufficiently high.[26] As the dangling bond of the HH1 hemihydride has identical properties to an isolated
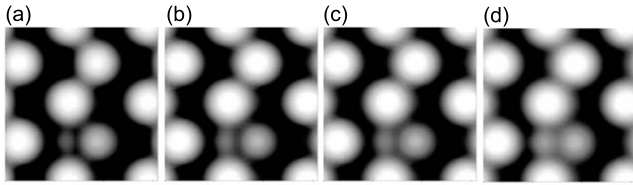
FIG. 11. Filled state ILDOS plots for the HH1 hemihydride configuration for a (4×4) surface unit cell for the integration ranges (a) -0.5 eV, (b) -1.0 eV, (c) -1.5 eV, and (d) -2.0 eV. All of these images are seen to be qualitatively the same.

dangling bond on hydrogenated Si(001), we conclude that charge accumulation on an electron-rich n-type substrate can lead to the localization of an electron on the isolated dangling bond of a hemihydride in the ground state HH1 configuration. This situation is illustrated in the experimental STM images shown in Fig. 2(a). In the following section, we will show that charge accumulation on an electron-rich n-type surface can be further increased by STM tip-induced downward band bending[27,28] and can lead to a reversible localization of electrons on the hemihydride in the HH1 configuration, as seen in our experimental data.

The bias-dependent appearance of the nonhydrogenated hemihydride Si atom can be observed in Fig. 2. The bright feature arising from the unsaturated Si atom of the Si-Si-H in the empty state images simply decreases in intensity relative to the Si atoms of the surrounding Si-Si dimers with increasing bias voltage [see Figs. 2(d) and 2(e)]. By contrast, the footprint of the Si-Si-H displayed in the filled state STM images changes significantly from a dark feature at low bias [Fig. 2(a)] to a bright feature at higher bias [Fig. 2(c)]. While the decreasing intensity of the hemihydride feature with increasing bias in the empty states is readily explained by the increasing contribution from the other states, the observed transition to a brighter image for the hemihydride at higher filled state bias cannot be explained in this way. This is evidenced by the ILDOS plots shown in Fig. 11. In this figure, we present results for the HH1 Si-Si-H configuration for integration ranges of -0.5, -1.0, -1.5, and -2.0 eV. It is clear that increasing the integration range (including more states) does not produce the transition from the dark to bright feature seen in Figs. 2(a)–2(c). To explain this behavior, we need to consider charge accumulation on the surface due to the tip-induced band bending and its effects on the atomic and electronic structures of a HHI hemihydride.

2. Bias-dependent simulated scanning tunneling microscopy images

a. Negative bias voltage. In order to investigate how the accumulated charge can modify the geometry of the hemihydrides, we have carried out geometry optimization calculations for both the HH1 and HH2 configurations in a (4×4) surface unit cell containing one and two additional electrons (see the Appendix). Following the earlier notation, we denote these systems as N_e+1 and N_e+2.

The calculated buckling angles and bond length values of the progressively charged hemihydrides following ionic relaxation are presented in Table II.

The HH2 configuration is seen to remain essentially unaffected by the addition of electrons, while the HH1 configuration progressively changes from a near planar ($\sim 2°$) hemihydride in the N_e case, to an upward buckling of the unsaturated hemihydride Si atom of $\sim -8°$ for the N_e+2 case. The Si-Si(H) dimer bond length also increases for the HH1 configuration from 2.41 Å (N_e) to 2.47 Å (N_e+2). As changes in the buckling angles and bond lengths indicate progressive population of the dangling bond orbital, we can conclude that the addition of electrons leads to charge localization for the HH1 configuration, but not for HH2.

The localization of charge for the HH1 configuration is clearly seen in the series of -1.0 eV simulated filled state STM images shown in Fig. 12. With the addition of electrons to the system, the nonhydrogenated Si atom hemihydride site is seen to change from a less bright feature in Fig. 12(a) to a significantly brighter appearance in Fig. 12(c). This progressive brightening with increasing bias is due to STM-induced charge accumulation on the unsaturated Si atom of the hemihydride enhanced by the upward relaxation of this atom. This behavior is in good agreement with the experimental data shown in Fig. 2.

The mechanism that leads to the localization of the additional electrons for the HH1 configuration can be elucidated by considering the electronic band structures for the N_e+1 and N_e+2 HH1 configurations shown in Fig. 13. Comparing with the neutral N_e system in Fig. 9(a), we see that for the N_e+1 case [Fig. 13(a)], the Fermi level has shifted up toward the flat unoccupied surface state (indicated by the empty
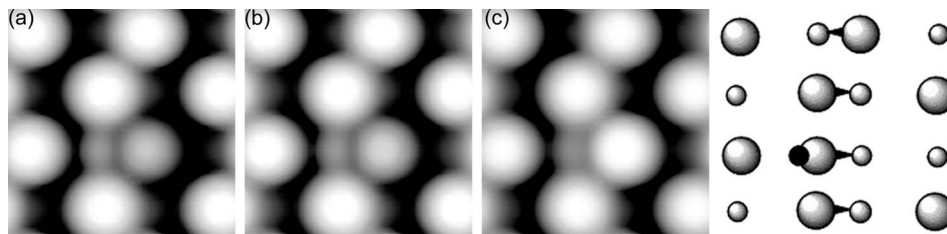

FIG. 12. Simulated filled state STM images (ILDOS plots) for a HH1 hemihydride: (a) one localized electron (N_e), (b) one localized electron (N_e+1), and (c) two localized electrons (N_e+2), calculated using a (4×4) surface unit cell and integrating over a range of 1.0 eV from the Fermi energy. The isosurface value was 2.7×10^{-4} e Å^{-3}. The right hand panel indicates the buckling of the Si-Si dimers and the initial (N_e) configuration of the Si-Si(H) dimer within the (4×4) surface unit cell.
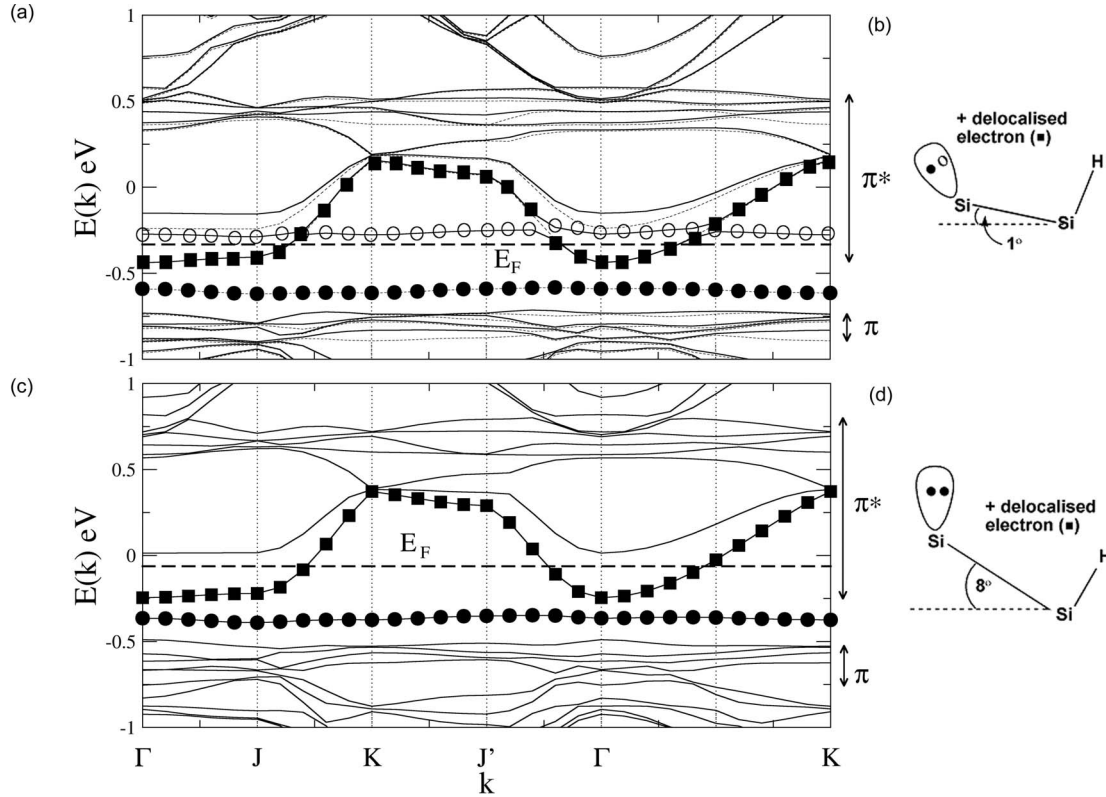
FIG. 13. Surface electronic band structures calculated using a (4×4) surface unit cell with six Si layers for the (a) N_e+1 and (c) N_e+2 charged HH1 configurations in the vicinity of the Fermi level (E_F). The hemihydride Si atom dangling bond states are indicated by the filled and empty circles. The filled squares denote the surface state partially occupied by the delocalized electron. Panels (b) and (d) present schematic configurations for the N_e+1 and N_e+2 charged HH1 structures, respectively.

circles) and now crosses one of the dispersive, low-energy surface states within the π^* band. The system has become metallic with the added electron being delocalized over the surface. The majority-spin dispersionless surface state below E_F [filled circles in Fig. 13(a)] remains occupied by one electron, while the minority-spin state (empty circles) remains unoccupied. It is the appearance of these localized states near E_F that leads to the observed STM appearance of the hemihydride at low negative bias and causes the susceptibility of the HH1 configuration to structural and electronic changes at high negative bias. In the N_e and N_e+1 cases, the half-occupied dangling bond of the unsaturated Si atom of the hemihydride appears less bright than that of the up-Si atoms of the neighboring bare Si-Si dimers. This gives rise to the relatively dark appearance of the hemihydride in the low-bias simulated image shown in Fig. 12(a). The increased brightness of the STM filled state appearance of the hemihydride in Fig. 12(c) results from changes in the geometry and

occupancy of the HH1 hemihydride dangling bond that are activated by the charge transfer into the empty localized state denoted by the empty circles in Fig. 13(a). Figure 13(c) for the N_e+2 system illustrates the effect of increased accumulated charge in the π^* band that occurs at high negative bias. The HH1 configuration remains metallic but the unoccupied minority-spin defect level associated with the hemihydride Si atom dangling bond has shifted downward in energy with respect to the π^* band and now lies below E_F so that the dispersionless surface state indicated by the filled circles becomes doubly degenerate. As a result, two electrons have now become localized on the hemihydride dangling bond orbital and the buckling of the hemihydride is reversed (see Table II). The simulated filled state STM image in Fig. 12(c) thus now shows the hemihydride Si atom to be very bright. This agrees well with the experimental high-bias filled state image in Fig. 2(c).

TABLE III. Hemihydride buckling angles (in deg) and bond lengths (in Å, given in parentheses) calculated for the HH1 and HH2 configurations with zero (N_e), one (N_e+1), two (N_e+2), three (N_e+3), and four (N_e+4) additional electrons for a (6×6) surface unit cell.

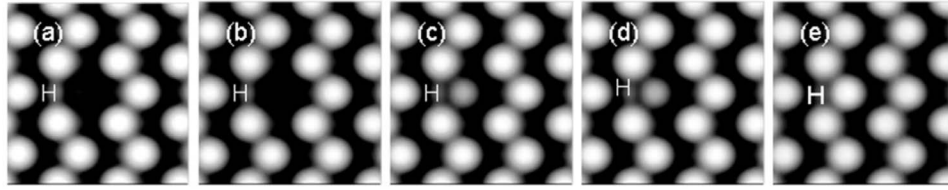|	N_e	N_e+1	N_e+2	N_e+3	N_e+4
HH1	8.5 (2.39)	7.2 (2.39)	0.4 (2.42)	−0.2(2.42)	−6.4(2.46)
HH2	10.0 (2.39)	9.9 (2.38)	9.9 (2.38)	9.9(2.37)	9.8(2.37)

FIG. 14. Simulated filled state STM images (ILDOS plots) for a HH1 hemihydride for a (6×6) surface unit cell and integrating over a range of -1.0 eV from the Fermi energy: (a) electron delocalized N_e, (b) electron delocalized N_e+1, (c) one localized electron N_e+2, (d) one localized electron N_e+3, and (e) two localized electrons N_e+4. The isosurface value was 2.7×10^{-4} e Å^{-3}.

Similar effects of the additional charge have been observed in our calculations carried out for the HH1 and HH2 configurations for the (6×6) surface unit cell (see Table III). The HH2 configuration for a (6×6) surface unit cell is seen to remain essentially unaffected by the addition of electrons. By contrast, the HH1 configuration is seen to change progressively from a positive buckling angle $(+8.5°, +7.2°)$ for N_e and N_e+1 to near planar $(+0.4°, -0.2°)$ for N_e+2 and N_e+3 and finally to a negative upward buckling of the unsaturated hemihydride Si atom of $-6.4°$ for N_e+4. The Si-Si(H) dimer bond length also increases from 2.39 Å (N_e) to 2.46 Å (N_e+4). As changes in the buckling angles and bond lengths indicate progressive population of the dangling bond orbital, we can again conclude that the addition of electrons leads to the charge localization for the HH1 configuration. The larger number of electrons needed to observe localization on the HH1 hemihydride for the (6×6) unit cell, when compared with the (4×4) cell, verifies that it is the charge density that is crucial in determining the localization or delocalization of charge.

This progressive localization of charge for the HH1 configuration and a (6×6) surface unit cell is clearly seen in the series of -1.0 eV ILDOS plots shown in Fig. 14. With the addition of electrons to the system, the nonhydrogenated Si atom hemihydride site is seen to change from a dark feature in Figs. 14(a) and 14(b) (no localized electrons) to a brighter feature in Figs. 14(c) and 14(d) (one localized electron) and then to a significantly brighter appearance in Fig. 14(e) (two localized electrons). This progressive brightening is due to the increasing density of surface electrons, analogous to the behavior of the HH1 configuration for a (4×4) surface unit cell shown in Fig. 12.

By contrast, the simulated filled state STM images calculated for the HH2 configuration and a (4×4) surface unit cell for the N_e+1 and N_e+2 cases (not shown here) remain essentially the same as for the neutral N_e system [Fig. 6(c)]. This is because the localized state associated with the dangling bond of the hemihydride for the HH2 configuration is too high in energy to be populated by the surface accumulated charge [see Fig. 5(a)]. The only significant difference seen in the electronic structure of the charged HH2 systems, from that shown in Fig. 5(a) for the neutral system, is a shift of E_F toward higher energies. The simulated filled state STM images thus remain virtually the same as that shown in Fig. 6(c) and are therefore inconsistent with the strong voltage dependence exhibited by the filled state experimental data [Figs. 2(a)–2(c)]. It follows that the bias-voltage-dependent

appearance of an isolated Si-Si-H hemihydride on an n-type Si(001) substrate that is seen in the experimental filled state topographs can only be explained by the properties of the HH1 configuration.

b. Positive bias simulated scanning tunneling microscopy images. At positive bias, the STM tip causes upward band bending and hence an overall depletion of electrons on the surface.[27,28] The calculated buckling angles and bond length values of the hemihydride for a (4×4) surface unit cell for such a case, namely, N_e-1, have already been presented in Table II. The hemihydride HH1 configuration was seen to change from a small downward buckling of the unsaturated hemihydride Si atom of $1.9°$ to $9.5°$, while the HH2 configuration remained virtually unchanged. The simulated STM images for the electron-deficient HH1 and HH2 configurations calculated for an integration range of $+0.2$ and $+1.0$ eV are shown in Fig. 15. We note that the $+1.0$ eV simulated image for the HH2 configuration [Fig. 15(d)] is significantly different from that obtained earlier for the neutral N_e case shown in Fig. 6(d). The downward-buckled atoms of the Si-Si dimers adjacent to the Si-Si-H hemihydride are now noticeably brighter than their upward—buckled partner Si atoms and the resulting simulated image is in good agreement with the experimental empty state STM images shown in Figs. 2(e) and 2(h). This image thus provides a significantly better representation of the experimental empty state data than the corresponding N_e simulation. The simulated image for the electron-deficient HH1 configuration in Fig.
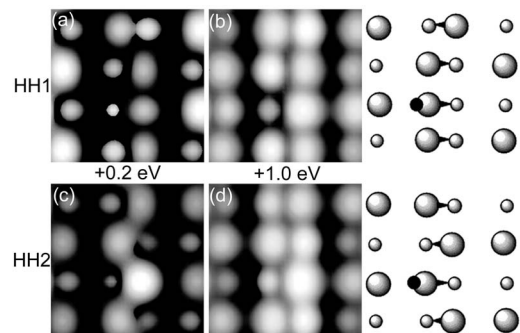

FIG. 15. Simulated empty state STM images (ILDOS plots) for the N_e-1 [(a) and (b)] HH1 and [(c) and (d)] HH2 configurations for a (4×4) surface unit cell, integrating over a range of [(a) and (c)] $+0.2$ eV and [(b) and (d)] $+1.0$ eV. The isosurface value was 2.7×10^{-4} e Å^{-3}. The right hand panels indicate the buckling of the Si-Si dimers and the N_e Si-Si-H hemihydride within the (4×4) surface unit cell.

15(b), on the other hand, is very similar qualitatively to that shown in Fig. 8(d) for the neutral case. This image thus also provides a good representation of the experimental empty state topographs in Figs. 2(e) and 2(h).

The +0.2 eV simulated STM images for the HH1 and HH2 N_e-1 configurations are shown in Figs. 15(a) and 15(c), respectively. We note that for this low integration range, the down-buckled Si atoms in the simulated STM images appear bright as is the common interpretation of low-bias empty state imaging.[24,25] While all of the unoccupied surface states contribute to the +1.0 eV simulated images, the ILDOS plots for +0.2 eV only include contributions from the bands just above the Fermi energy. In this case, the simulated images for HH1 and HH2 are seen to be quite different, and only the latter image (HH2) reproduces the buckling of the Si-Si dimers seen in the experimental images [see Fig. 2(h)]. We can thus conclude that when charge depletion is taken into account, and all of the surface states are integrated, both configurations are consistent with the experimental STM images of the Si-Si-H hemihydride measured at positive bias. Including only the empty surface states lying very close to the Fermi energy, on the other hand, suggests a preference for the lower-energy HH2 configuration.

IV. DISCUSSION AND CONCLUSIONS

In this paper, we have studied the nature of the isolated Si dangling bond that results from the chemisorption of a single hydrogen atom on Si(001) and the formation of a Si-Si-H hemihydride. Our calculations show that two different stable atomic configurations exist for the hemihydride system. We have further shown that the localization or delocalization of the surface charge on the isolated Si dangling bond of the hemihydride is correlated with the buckling angle of the Si-Si(H) dimer, the size of the surface unit cell, and the configuration (whether parallel or antiparallel) of the surrounding bare Si-Si dimers. Experimentally, it is well known that the electrostatic effect of an STM tip is to induce band bending and hence a shift in the surface bands with respect to the Fermi level.[27,28] This shift of the surface states relative to E_F leads to charging of the surface, which, in turn, leads to charging of the localized dangling bond orbital of the unhydrogenated Si atom of the hemihydride and local structural changes. These effects are essential to explain the complex negative bias-voltage-dependent STM appearance of an isolated hemihydride on *n*-type Si(001).

Both the appearance of the filled state images and their observed bias dependence show that the structure that is observed in the experimental data for negative sample bias originates from the parallel HH1 configuration. However, at high negative bias, the buckling of this HH1 configuration is reversed so that the actual buckling of the Si-Si dimers adjacent to the Si-Si-H hemihydride constitutes an antiparallel configuration. Moreover, both the HH1 and HH2 configurations have been found to be consistent with the experimental empty state STM images, with the HH2 configuration being preferred at low positive bias. It thus follows that the appearance of the hemihydride for positive and high negative biases can be explained by the hemihydride and its adjacent bare

Si-Si dimers in the same dimer row forming an "antiparallel" dimer configuration. This is intuitively what one would expect as such configurations are well known to reduce the surface strain, and indeed our calculations determined the uncharged HH2 configuration to be lower in energy than HH1. The puzzling feature, however, is the appearance of the HH1 parallel hemihydride configuration at low negative bias voltage. At negative bias voltage, tip-induced band bending results in an accumulation of charge on the surface. To explain the observation of the HH1 parallel configuration at low negative bias voltage, we thus need to determine the relative energies of the HH1 and HH2 configurations with increasing charge. Unfortunately, we cannot obtain accurate energies for the HH1 and HH2 charged systems from the VASP code, and hence a direct comparison of the relative energies of these two configurations with increasing charge is not possible. Resolution of why the HH1 configuration is the preferred configuration at low negative bias must therefore await the development of a reliable theoretical method for determining the energetics of charged semiconductor-adsorbate systems.

As we have seen, the electronic structure near E_F of the Si-Si-H hemihydride is dominated by the creation of an isolated Si dangling bond. The Si-Si-H hemihydride is thus a prototype system for a broad range of adsorbate systems on Si(001) that create single unpaired dangling bonds. This includes systems such as those involving F, Cl, I, and OH.[29–31] The results discussed in this paper should therefore be relevant to many other systems. It is important in this context to recall that we have obtained similar experimental and theoretical results to those reported here for an isolated Si-P heterodimer on Si(001).[14] In this case, a phosphorus atom substitutes for one of the silicon atoms of a surface Si-Si dimer to form a Si-P heterodimer. This heterodimer has an isolated dangling bond on its Si atom and thus may be regarded as isoelectronic to a Si-Si-H hemihydride. The negative bias-voltage dependence of the STM images was shown to result from filling the dangling bond orbital of the heterodimer Si atom produced by a tip-induced shift in the Fermi energy, analogous to the mechanism proposed here for the Si-Si-H. In both cases, the buckling sequence and bias dependence of the filled states can only be explained in terms of the higher-energy parallel configuration.

APPENDIX: ESTIMATE OF THE TOTAL CHARGE ACCUMULATED UNDER AN APPLIED BIAS VOLTAGE *V*

Theoretical modeling of the effects of a metallic tip near the surface of a semiconductor has been attempted by several

authors (see the references in Ref. 32). These models, which are based on Poisson's equation and the application of appropriate continuity conditions, allow the electrostatic potential and induced charge density to be approximated but are somewhat complicated in that they generally require the solution of self-consistent equations. In the following, we present a very simple derivation, which enables us to determine a rough estimate of the total charge Q that would be accumulated near a surface as the result of an applied tip bias voltage V. To determine this estimate for Q, we make the following assumptions:

(i) The diameter of the tip (10–25 nm) is sufficiently large that there is a constant electric field $E = V/d$ normal to the surface (the z direction), where V is the applied bias voltage and d is the tip-surface separation.

(ii) $\rho(x,y,z)$ is constant in the x and y directions.

(iii) Electrons in the surface region will redistribute under the influence of the bias voltage until the induced electric field exactly balances the applied field creating the charge redistribution.

Using these assumptions, Poisson's equation,

$$\nabla^2 V(x,y,z) = -\rho(x,y,z)/\varepsilon,$$

reduces to

$$\frac{d^2 V}{dz^2} = -\rho(x,y,z)/\varepsilon,$$

where $V(x,y,z)$ is the potential associated with the additional charge density $\rho(x,y,z)$ and ε is the dielectric constant of the substrate.

Integrating this with respect to z, where $z = 0$ defines the surface, yields

$$E(z)|_{z=-\infty}^{z=0} = E(0) - E(-\infty) = E(0) = \int_{-\infty}^{0} \rho(x,y,z)dz/\varepsilon.$$

The total accumulated charge Q in a unit cell of surface area A is then given by

$$Q = A \int_{-\infty}^{0} \rho(x,y,z)dz = A\varepsilon E(0) = A\varepsilon V/d.$$

For $\varepsilon = 5\varepsilon_0$, $d = 7$ Å, and a (4×4) surface unit cell of side 1.54 nm [Si(001)], this yields the result

$$Q = 0.94 V e.$$

This predicts that a bias voltage of 1 V would result in an accumulated charge of around one electron.

[1] J. M. Buriak, Chem. Rev. (Washington, D.C.) **102**, 1272 (2002).
[2] T. C. Shen, C. Wang, G. C. Abeln, J. R. Tucker, J. W. Lyding, P. Avouris, and R. E. Walkup, Science **268**, 1590 (1995).
[3] J. W. Lyding, T. C. Shen, J. S. Hubacek, J. R. Tucker, and G. C. Abeln, Appl. Phys. Lett. **64**, 2010 (1994).
[4] S. R. Schofield, N. J. Curson, M. Y. Simmons, F. J. Ruess, T. Hallam, L. Oberbeck, and R. G. Clark, Phys. Rev. Lett. **91**, 136104 (2003).
[5] J. E. Buehler and J. J. Boland, Science **200**, 506 (2000).
[6] J. J. Boland, Phys. Rev. Lett. **67**, 1539 (1991).
[7] J. J. Boland, J. Vac. Sci. Technol. A **10**, 2458 (1991).
[8] S. Watanabe, Y. A. Ono, T. Hashizume, and Y. Wada, Phys. Rev. B **54**, R17308 (1996).
[9] T. Hashizume, S. Heike, T. Higosugi, and K. Kitazawa, in *Advances in Scanning Probe Microscopy*, edited by T. Sakurai and Y. Watanabe (Springer-Verlag, Berlin, 1996).
[10] K. Bobrov, G. Comtet, G. Dujardin, and L. Hellner, Phys. Rev. Lett. **86**, 2633 (2001).
[11] E. Hill, B. Freelon, and E. Ganz, Phys. Rev. B **60**, 15896 (1999).
[12] D. R. Bowler, J. H. G. Owen, C. M. Goringe, K. Miki, and G. A. D. Briggs, J. Phys.: Condens. Matter **12**, 7655 (2000).
[13] J. van Heys and E. Pehlke, Phys. Rev. B **72**, 125351 (2005).
[14] M. W. Radny, P. V. Smith, T. C. G. Reusch, O. Warschkow, N. A. Marks, H. F. Wilson, N. J. Curson, S. R. Schofield, D. R. McKenzie, and M. Y. Simmons, Phys. Rev. B **74**, 113311 (2006).
[15] M. A. Filler and S. F. Bent, Prog. Surf. Sci. **73**, 1 (2003).
[16] G. Kresse and J. Hafner, Phys. Rev. B **47**, 558 (1993); **49**, 14251 (1994).
[17] G. Kresse and J. Furthmuller, Comput. Mater. Sci. **6**, 15 (1996).
[18] G. Kresse and J. Furthmuller, Phys. Rev. B **54**, 11169 (1996).
[19] D. Vanderbilt, Phys. Rev. B **41**, 7892 (1990).
[20] J. P. Perdew, J. A. Chevary, S. H. Vosko, K. A. Jackson, M. R. Pederson, D. J. Singh, and C. Fiolhais, Phys. Rev. B **46**, 6671 (1992).
[21] J. Tersoff and D. R. Hamann, Phys. Rev. Lett. **50**, 1998 (1983).
[22] J. Tersoff and D. R. Hamann, Phys. Rev. B **31**, 805 (1985).
[23] K. Hata, S. Yasuda, and H. Shigekawa, Phys. Rev. B **60**, 8164 (1999).
[24] J. Ihm, M. L. Cohen, and D. J. Chadi, Phys. Rev. B **21**, 4592 (1980).
[25] This effect has been reported for the clean Si(001) surface by Hata *et al.* (Ref. 23) who found that the up-Si dimer atoms imaged brightly in the experimental empty state STM images at bias voltages greater than 2 V.
[26] P. G. Piva, G. A. DiLabio, J. L. Pitters, J. Zikovsky, M. Rezeq, S. Dogel, W. A. Hofer, and R. A. Wolkow, Nature (London) **435**, 658 (2005).
[27] R. M. Feenstra, J. Vac. Sci. Technol. B **5**, 923 (1987).
[28] G. W. Brown, H. Grube, M. E. Hawley, S. R. Schofield, N. J. Curson, M. Y. Simmons, and R. G. Clark, J. Appl. Phys. **92**, 820 (2002).
[29] A. Vittadini, A. Selloni, and M. Casarin, Phys. Rev. B **52**, 5885 (1995).
[30] G. J. Xu, Surf. Sci. **577**, 77 (2005).
[31] J. J. Boland, Science **262**, 1703 (1993).
[32] R. M. Feenstra, J. Vac. Sci. Technol. B **21**, 2080 (2003).